LBL-27073
Preprint

Lawrence Berkeley Laboratory
UNIVERSITY OF CALIFORNIA

Materials & Chemical Sciences Division

National Center for Electron Microscopy

Submitted to Acta Metallurgica

RECEIVED
LAWRENCE
BERKELEY LABORATORY

JUL 31 1989

LIBRARY AND
DOCUMENTS SECTION

The Martensitic Transformation in Silicon
III. Comparison with Other Work

P. Pirouz, U. Dahmen, and K.H. Westmacott, and R. Chaim

April 1989

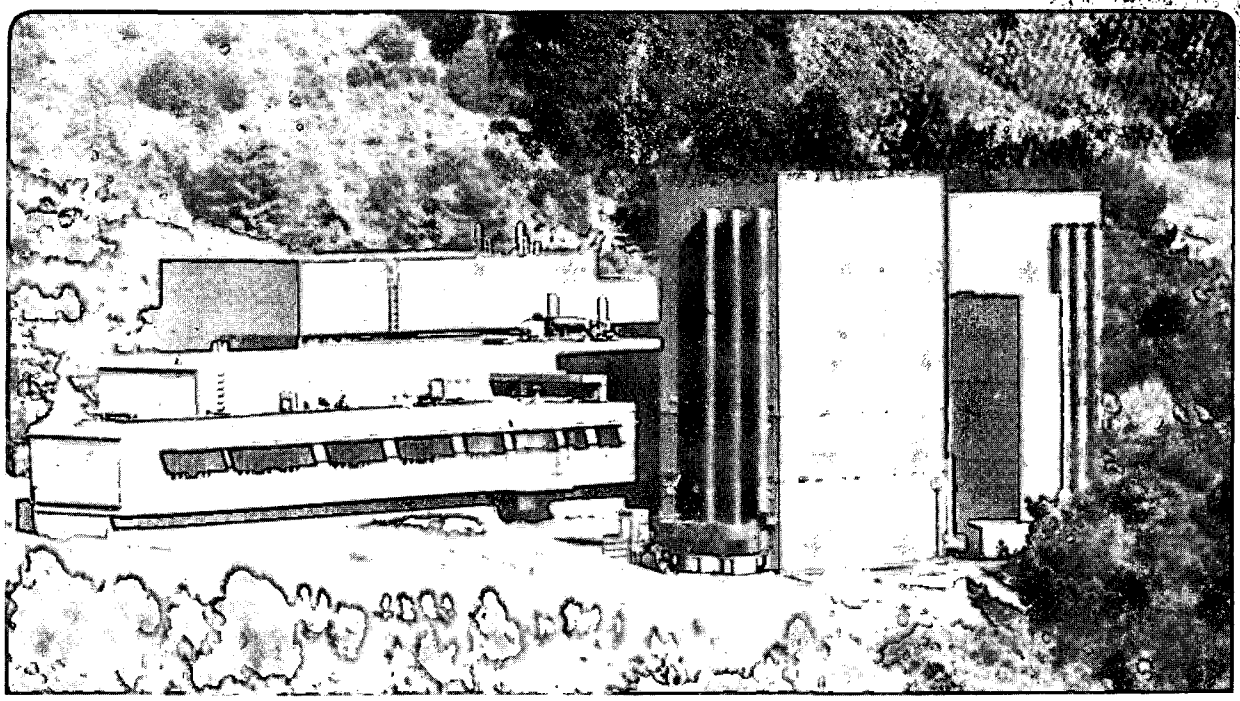

LBL-27073 c.2

Prepared for the U.S. Department of Energy under Contract Number DE-AC03-76SF00098.

DISCLAIMER

This document was prepared as an account of work sponsored by the United States Government. While this document is believed to contain correct information, neither the United States Government nor any agency thereof, nor the Regents of the University of California, nor any of their employees, makes any warranty, express or implied, or assumes any legal responsibility for the accuracy, completeness, or usefulness of any information, apparatus, product, or process disclosed, or represents that its use would not infringe privately owned rights. Reference herein to any specific commercial product, process, or service by its trade name, trademark, manufacturer, or otherwise, does not necessarily constitute or imply its endorsement, recommendation, or favoring by the United States Government or any agency thereof, or the Regents of the University of California. The views and opinions of authors expressed herein do not necessarily state or reflect those of the United States Government or any agency thereof or the Regents of the University of California.

LBL-27073

The Martensitic Transformation in Silicon
III. Comparison with Other Work

P. Pirouz,[1] U. Dahmen,[2] K.H. Westmacott,[2]
and R. Chaim[1]

[1]Department of Materials Science and Engineering
Case Western Reserve University
Cleveland, Ohio 44106

[2]National Center for Electron Microscopy
Materials and Chemical Sciences Division
Lawrence Berkeley Laboratory
1 Cyclotron Road
Berkeley, California 94720

April 1989

The Martensitic Transformation in Silicon

III) Comparison With Other Work

P. Pirouz[1], U. Dahmen[2], K. H. Westmacott[2], and R. Chaim[1*]

[1] Department of Materials Science and Engineering, Case Western Reserve University, Cleveland, OH 44106.

[2] National Center for Electron Microscopy, Lawrence Berkeley Laboratory, University of California, Berkeley, CA 94720.

ABSTRACT

In the previous papers, [1,2], the experimental observations on the cubic→hexagonal phase transformation in silicon were presented and a crystallographic analysis was given which explained this transformation on the basis of lattice accommodation in twin-twin interactions or propagation of secondary twins into the matrix. In the present paper, the martensitic nature of the transformation is discussed and other recent observations of hexagonal silicon in ion-implanted material, heat treated Czochralski Si, and silicon deformed under hydrostatic pressure are considered in the light of the present work.

1. INTRODUCTION

High resolution observations have unequivocally confirmed earlier reports of a hexagonal phase of silicon formed by hot indentation. Paper I [1] of this series gives a detailed account of these new results. In paper II [2], an analysis relates the transformation to multiple twinning and martensite crystallography. A detailed discussion of related hexagonal and other phases, and possible formation mechanisms, are the subjects of this final paper.

2. MARTENSITIC NATURE OF THE TRANSFORMATION

Although the dh phase in silicon is not a thermodynamically stable phase, the diffusionless mechanism by which it forms and its crystallographic characteristics make the dc→dh transformation a martensitic one.

In general, a martensitic transformation occurs because a particular structure becomes thermodynamically unstable. It usually involves shape changes occurring in narrow plates within a constraining matrix. Because of this, and also as a result of a cooperative and diffusionless reaction, a martensitic transformation involves a substantial amount of strain energy. Hence to nucleate such a transformation, a large driving force is required. Two ways in which sufficient driving forces for the martensitic transformation can be built up without the onset of diffusional processes are rapid cooling and high strain rates. With sufficiently rapid cooling through the thermodynamic region in which the matrix is unstable, there is often not enough time for diffusional processes to take place and the large undercooling provides a large enough driving force for the martensitic transformation to occur (e.g. the austenite→martensite transformation in steel). At temperatures where the undercooling is not sufficient for a large driving force, the application of applied stresses at a high rate again builds up enough driving force to carry through a martensitic transformation. There are a number of systems in which the martensitic transformation is stress induced, e.g. the tetragonal→monoclinic transformation in zirconia. Indentation, of course, involves the application of very large stresses at very high strain rates.

The crystallographic theory of martensitic transformation is phenomenological since it describes the crystallography before and after the transformation, but not the path it takes. The path or mechanism of a martensitic transformation has been the subject of much controversy especially for the case of the fcc→bcc transition. Many authors have suggested mechanisms that amount to different decompositions of the transformation strain (e.g. [3-9]) and can be described in terms of different partial dislocation reactions. However, which particular mechanism operates can only be decided by experiment, and as the decisive experiments are hard to design the controversy remains unresolved. Perhaps the most informative experimental data are to be found in premartensitic phenomena which indicate a lattice softening on a specific shear system.

The situation is simplest in the fcc→hcp transformation where experimental observations show the mechanism to be one in which Shockley partial dislocations propagate on every other close packed plane. However, as pointed out earlier, the cubic to hexagonal transformation in Si has a distinctly different crystallography and it cannot be achieved by this simple mechanism. The question of a mechanism in Si is in fact much more closely related to the fcc→bcc transformation. From Fig. 3(a) in part II [2], the atomic displacements can be seen to be a simple shear (plus a

shuffle). In terms of dislocations, the 1/6 <112> partials on {111} planes that produce the secondary twin become 1/18 <255> partials on {511} planes when they enter the matrix. Since {511} planes have only one third the interplanar spacing of {111} planes, these dislocations would be further dissociated into 1/64 <255> partials on every {511} plane (rather than 1/18 <255> on every third {511} plane). Because of the loose packing and close spacing of {511} planes it is difficult to imagine this shear as a physically meaningful dislocation mechanism. It is therefore tempting to search for alternative mechanisms that involve more acceptable partial dislocations such as the 1/6 <112> Shockleys. However, it must be kept in mind that whatever combination of these dislocations is chosen, the net result must be the atomic displacements shown in Fig. 3(a) of part II [2]. Thus, any alternative dislocation mechanism could only be a less direct route to the same final state. In section 2 of part II [2] the total displacement was decomposed into a lattice rotation (the 39° rotation of a secondary twin relative to the matrix) and an accommodation shear (the reverse twinning shear).

In terms of a dislocation mechanism, it is most appropriate to consider the model of intersecting twins. Each twin would be formed by the mechanism of Ref. [10] which is based on the different mobility of partial dislocations in silicon [11]. This difference is due to the different activation energies for glide of the leading and trailing partials of a dissociated screw dislocation and it increases with decreasing temperature. According to the model, three ingredients are necessary for occurrence of twinning in silicon: (1) a pinned segment of screw dislocation, (2) shear stresses acting on the dislocation segment on the primary *and* a cross-slip plane, and (3) intermediate temperatures. It is envisaged that all three ingredients are present in the complex stress field of an indentation test and a high density of twins with different {111} habit planes form.

Consider now the intersection of two twins, 1 and 2, formed in this way on different habit planes. When twin 2 reaches twin 1, transformation of the partials to 1/18 <255> represents only one of many possibilities. In another decomposition of the strain, the reaction would be expressed in terms of the more familiar Shockley partial dislocations. It is postulated that under the high local stresses, coalescence of the Shockley partials on adjacent planes can occur at the interface of the twins. Once three such partials have collected at the boundary, their coalescence will form a dislocation with an effective Burgers vector 1/6 $[\bar{5}\,5\bar{2}]_{T1}$ which subsequently dissociates as follows [12]:

$$1/6\,[\bar{5}\,5\bar{2}]_{T1} \rightarrow 2\times 1/6\,[\bar{1}\,12]_{(\bar{1}1\bar{1})} + 3\times 1/6\,[\bar{1}\,1\bar{2}]_{(\bar{1}11)}$$

It should be noted, however, that the strict propagation sequence necessary to accomplish the transformation is not readily visualized.

Still other decompositions are possible, and each has its own dislocation description. To decide which is the one that actually describes the mechanism of transformation is a question to be answered not by theory but by experiment. If it were possible to unravel the dislocation structure at an advancing (or receding) interface it could be determined whether the transformation proceeds by the propagation of 1/64 <255> dislocations on successive {511} planes, by a more complex sequence of Shockley partials on different slip planes, or an even different set of dislocations or shuffles.

3. RELATED PHASES AND OTHER OBSERVATIONS OF HEXAGONAL SILICON

3.1. High Pressure Phases of Silicon

As noted earlier, the room temperature diamond cubic structure of silicon persists up to ~11 GPa, and at atmospheric pressure, from 0 K to its melting point. Using Cannon's designation [13], the dc silicon is known as the Si(I) phase. Other high pressure phases of Si are designated as follows [14]:

Si (II) --- between 11-15 GPa, a metallic phase with the body centered tetragonal (bct) structure, [15,16],

Si (III) --- between 10 and 0 GPa, a body centered cubic (bcc) phase [17,18],

Si (IV) --- a similar quenched phase of Si(III) [13,14],

Si (V) --- between 14 and 40 GPa, a primitive hexagonal (ph) phase [19,20],

Si (VI) --- an intermediate phase of unknown structure [19],

Si (VII) --- at ~40 GPa, a hexagonal close packed (hcp) phase [19].

According to recent work by Hu and Spain [20], with increasing pressure up to ~25 GPa, the sequence of transitions is I → II → V. It should be noted that there is no sharp transition pressure in the above sequence and two-phase regions exist over wide ranges of pressure [20]. On release of the pressure, the phase transitions follow the sequence V → (V+II) → II → (II+III) → III with the bcc phase persisting to atmospheric pressure [20].

In addition to these pressure-induced phase transformations, which are accompanied by a large volume decrease, a diamond hexagonal (dh) form of silicon was first reported in the high-pressure experiments of Wentorf and Kasper [17]. Extensive heat-treatments of the polyphase (dc+bcc) silicon, obtained under high pressure, at temperatures of 200-600° C for periods of between 30 minutes and 3 days produced a mixture of dc silicon and a new phase. Using Debye-Scherrer X-ray patterns, Wentorf and Kasper determined this new phase to be hexagonal, and as they stated,

"corresponding to a structure related to the wurtzite type in the same way that the structure of ordinary silicon is related to the zincblende type" [17]. The lattice parameters of the dh silicon were a=0.38 nm and c=0.628 nm, i.e. c/a=1.653, close to the ideal value of $(8/3)^{1/2}$. It had the same density, 2330 kg/m^3, as that of dc silicon implying that unlike the high-pressure phases, dh Si has an identical atomic volume to that of dc silicon. The new phase showed semiconducting properties with a resistivity of 100 Ωm which decreased sharply with increasing temperature. This compares to a resistivity of 10^{-3}-10^{-4} Ωm for the bcc silicon, which shows metallic behavior, and has a lattice parameter of 0.6636 nm and a density of 2550 kg/m^3 [18].

The dh structure has the space group $P6_3/mmc$ with four atoms per unit cell at 0,0,0; 0,0,3/8; 2/3,1/3,1/2 and 2/3,1/3,7/8. It has tetrahedral bonding similar to that of dc Si with a coordination number of 4; the only difference is in the positions of the third nearest neighbors.

The phase stabilities in silicon have also been the subject of intense theoretical study. In particular, Yin and Cohen [21,22] investigated the static structural properties (e.g. lattice constant, cohesive energy, bulk modulus), crystal stability and pressure-induced phase transformations in silicon on the basis of ab initio pseudopotential method within the local density-functional formalism. Their method is based on the calculation and comparison of the total energy of various plausible crystalline structures (fcc, bcc, hcp, dc, dh, bct and simple cubic) for silicon as a function of volume. The theoretical values of the structural properties of Si obtained by Yin and Cohen [21,22] are in excellent agreement with the experimental values. They find that, out of the seven crystal structures that they considered, the dc and dh Si are semiconducting with strongly covalent bonding characteristics, and the other five structures are metallic. According to their results, under atmospheric pressure, dc silicon has the lowest structural energy as expected; however, the difference in the structural energy between dh silicon and dc silicon is very slight (0.016 eV per atom). It seems that only the slightly more localized charge distribution in dh Si makes this phase less stable than the dc phase [22]. Their results also show that dh Si is not a thermodynamically stable phase and dc silicon cannot transform to dh silicon at equilibrium under any pressure. Thus, unlike other forms of silicon, with the exception of Si(III), the dh phase seems to be metastable over the whole pressure range with an energy curve lying slightly higher than that of dc Si [23].

3.2 Related Hexagonal Phases

It is of relevance to the present discussion to mention briefly the observation of a similar hexagonal phase in other group IV materials: diamond and germanium.

3.2.1 Hexagonal Diamond

The dh form of diamond is called Lonsdaleite; a name suggested by Frondel and Marvin [24] after the crystallographer Dame Kathleen Lonsdale. It was first reported in experiments on the production of synthetic diamond by shock compression of graphite finely dispersed in a metallic shock plate [25]. Bundy and Kasper [26] synthesized hexagonal diamond by compression along the c-axis of good single-crystal graphite with a subsequent stabilization through heating above 1000°C under high

pressure. Using the Debye-Scherrer x-ray powder method, they measured the lattice parameter of the hexagonal phase to be a=0.252 nm and c/a=1.63 with the new phase having the same density as cubic diamond. Significantly, they also reported that the crystals were twinned and that they had the following orientation relationship to the original graphite crystal:

$$(10\bar{1}0)_{dh} \,||\, (0001)_{graphite}$$
$$[0001]_{dh} \,||\, [11\bar{2}0)_{graphite} \qquad ....(1)$$

As they commented, the graphitic structure cannot be converted to the dh structure by simple shear processes and would require atomic displacements (shuffling). Lonsdale suggested that this transformation is partly because of the greater ease of transition of the sequence $(0001)_{graphite}$ to $(10\bar{1}0)_{dh}$ as compared to alternative transitions [27]. However, it is likely that the tranformation of the graphite to the dh diamond was a two-stage process: first a high pressure phase transformation of graphite to cubic diamond with a subsequent formation of dh diamond by the double twinning mechanism outlined in part II [2]. In the first stage, graphite undergoes a phase transformation to dc diamond with the usual orientation relationship of:

$$(0001)_{graphite} \,||\, (111)_{dc}$$
$$[11\bar{2}0]_{graphite} \,||\, [1\bar{1}0]_{dc} \qquad ....(2)$$

The second stage now results in dh diamond with the following orientation relationship:

$$(0\bar{1}1)_{dc} \,||\, (0001)_{dh}$$
$$[011]_{dc} \,||\, [\bar{1}2\bar{1}0]_{dh} \qquad ....(3)$$

Note also that the c/a ratio in this case is very close to the ideal ratio of $(8/3)^{1/2}$.

The dh phase of diamond was also reported in Canyon Diablo iron meteorites by Frondel and Marvin [24] and by Hanneman et al. [28]. The latter also observed dh diamond in Goalpara meteorites. According to Hanneman et al. [28], their evidence indicates that cubic diamond cannot be transformed, even partially, into hexagonal diamond by application of static or shock pressure combined with temperature. However, the dh phase of diamond in meteorites could have formed by the martensitic transformation suggested here.

3.2.2 Hexagonal Germanium

The dh germanium was first observed by Eremenko [29] using the same indentation technique as the one that he had used on silicon [30,31]. The optimum range of indentation temperature for the production of hexagonal Ge was found to be ~380-400° C and all the crystallographic data, e.g. the habit plane and the orientation relationship between Ge_{dh} and Ge_{dc}, were similar to the silicon case. According to Eremenko, the germanium dh phase essentially could not be observed below ~150° C and above ~550° C. The lattice parameter was a=0.394±0.005 nm with c/a=1.66.

Rudee and Howie [32] investigated sputtered Ge using HREM and found it to have a microcrystalline structure rather than an amorphous one. They found excellent agreement between the experimental diffraction patterns of the sputtered Ge and those calculated from dh Ge. Later, Parsons and Hoelke [33], also using HREM, observed dh Ge when a thin foil of the amorphous material was crystallized by a pulsed laser beam, by an electron beam, or by vacuum annealing. However, while the value of the lattice parameter reported by these authors (a=0.396±0.002 nm) was in

agreement, the c/a ratio (c/a=2.47), was markedly different from that reported by Eremenko [29]. Parsons and Hoelke [34] reported numerous defects, particularly microtwins, in the explosively crystallized (amorphous) films. Thus it is possible that the dh Ge observed in these specimens arises by one of the mechanisms described in part II [2], e.g. from the intersection of twins. In any case, verification of dh Ge by such experiments, and determination of lattice parameters, needs re-evaluation.

3.3. Hexagonal Phase in Ion-Implanted Silicon

The first observation of hexagonal silicon in ion-implanted Si was made by Tan et al. [35]. Their experiment was on silicon wafers implanted with high doses of As^+ ions with an estimated temperature below "a few hundred degrees Celsius" [35]. They stated that the hexagonal Si that they observed was not the same defect as the previously reported rod-like defects or {111} stacking faults also generated during ion implantation of Si.

Since the work of Tan et al., the hexagonal phase has been reported a number of times when silicon is implanted by a heavy ion dose ($\sim 10^{21}$-10^{22} ions/m^2) of As^+ [36], Ar^+ [37], Kr^+ [38], and P^+ [39]. There are also indications that in earlier studies this phase had been observed. For example, Schwuttke et al. [40] investigated Si^+-implanted (111) silicon by TEM and the diffraction patterns in their paper show spots which may be due to the hexagonal phase; the authors actually indexed these spot as hexagonal reflections although they attributed them to stacking faults parallel to the substrate {111} plane. Similarly Ohdomari and Onoda [41] analysed the diffraction patterns from Ar^+-implanted Si and noted anomalous spots which they attributed to multiply twinned particles.

In general, heavy ion implantation results in extensive radiation damage and amorphisation of silicon [42]. Depending on the mass, energy, and dosage of the implanted ions, the amorphous layer may extend from the implanted surface to a certain depth, or it may be buried under a crystalline region [43]. The formation of amorphous silicon is a result of the damage produced by the implanted ions which create a high density of point defects through knock-on processes. During the implantation process, however, the damaged crystal is being annealed resulting in a recovery of some of the damage and recrystallization of the amorphous regions. This latter process, termed "dynamic annealing", is clearly thermally activated and thus a function of the specimen temperature. Thus, the extent of the damage produced in ion implantation of a crystalline material is determined by the competition between two simultaneous processes: (i) defect production, and (ii) dynamic annealing [37,44]. At low temperatures, the rate of thermal annealing is less than the rate of damage production and net amorphisation takes place. At high temperatures, the situation is reversed and net recrystallization occurs. Depending on the dose, on a single crystal substrate, the reordered silicon may grow in an epitaxial orientation relationship with respect to the non-amorphized region [42]. Since the material which transforms, i.e. amorphous silicon, is also in the solid phase, the whole recrystallization process is termed "solid-phase epitaxial growth" (SPEG) to distinguish it from vapor- or liquid-phase epitaxial growth. The temperatures at which SPEG occurs in silicon is generally above 450° C [44]. Such temperatures can be achieved in heavy implantations since the high

current used for this purpose can increase the temperature of the specimen by an appreciable amount [43]. This is specially the case when there is poor thermal contact with the specimen holder. The amorphous/crystalline interface during the annealing process depends on the initial orientation of the silicon, e.g. in {100} or {110} implantations, the interface seems to be quite planar while in the {111} case it is rather non-uniform [45-47].

There is ample experimental evidence that ion implantation of silicon with dynamic annealing [35,37-39,48], or post-implantation annealing [36,37,40,41,43,46,50], produces extensive twinning in the recrystallized region. Both primary and secondary microtwins occur which apparently form during the recrystallization of the amorphous phase [37,42]. In fact, Cspregi et al. [47] ascribe the bilinear mode of the recrystallization growth curve for <111> oriented silicon to the growth of twins in this direction during recrystallization. The microtwins often have the shape of small plates with widths in the range of 10-30 nm [37].

More recently, it has been found that post-implantation annealing of silicon which contains an amorphous layer can be assisted by a secondary irradiation [49]. Thus irradiation with energetic ions induces recrystallization at temperatures as low as 200° C [44]. Interestingly, in the ion-induced recrystallization of amorphous silicon, which occurs at temperatures below 400° C, there is no evidence of twins or hexagonal phase [50].

Formation of twins and hexagonal phase in ion-implanted silicon can be explained on the basis of the models developed in the present series of papers. First it should be noted that if a pinned screw dislocation is under a shear stress, then passing through the temperature range 400-650° C, say on heating up to higher temperatures, can activate the glide of the leading partial dislocation to a much greater extent than that of the trailing partial. Hence, provided there is sufficient shear stress acting on the partial dislocation on the cross-slip plane, a twin lamellae can be produced in this temperature range. Now, during the recrystallization process, internal shear stresses are produced in the implanted material. These may be due to a variety of reasons, e.g. the implanted ion may not be soluble, or be above its solubility limit, in silicon. In this case, the ions will precipitate out as second-phase particles during dynamic, or post-implantation, annealing processes with a different volume-per-atom to that of silicon, hence producing local stresses. For instance, Komarov et al. [50] attribute local stresses in Ar^+-implanted Si to formation of Ar bubbles which subsequently crystallize. In any case, the amorphous→crystalline phase transformation generates considerable stresses in the implanted layer due to different density of the two phases. As a result, dislocations loops nucleate heterogeneously at the many inhomogeneous sites present particularly close to the amorphous/crystalline interfacial regions. However, glide of dislocations is a thermally activated process with an activation energy of ~2 eV in silicon (this depends on the dopant concentration; for a recent review see [51]). Thus, at low temperatures, the mobility of dislocations is very low and, even though the embryonic dislocation loops nucleated at the heterogeneities are under considerable shear stress, they stay rather small because they cannot expand and shear the crystal. As the temperature rises in the specimen, the mobility of dislocations gradually increases and they start expanding. Segments of some screw dislocations are pinned by the various defects in this region of the crystal. Those segments whose leading partial

is faster than the trailing partial will now generate twins to relieve some of the shear stress acting on them. Once the twin is generated, rising temperature simply results in further expansion of the faulted loops on adjacent {111} planes and widening of the twin. This is the process that is thought to operate in the generation of twins.

Even though the stress field in an implanted layer is thought to be relatively simple [52], it can become quite complicated during the amorphous→crystalline phase transformation. Hence, there are likely to be dislocations generated on many different slip planes. Also there may be sufficient resolved shear stresses on these {111} planes to cause formation of twins with different {111} habit planes. If the twins with different habit planes intersect during their expansion, they can form hexagonal silicon by the mechanism described in part II of this series [2]. Since the resolved shear stress on different {111} planes is a function of the orientation of the substrate, it is expected that the twin density on different {111} planes, and as a result also the density of hexagonal silicon, will be different when different substrate orientations are implanted.

The absence of twins, and hence hexagonal silicon, in the ion-assisted experiments [50] is due to the fact that recrystallization takes place at such low temperatures ($<400^\circ$ C) that the partial dislocations are not sufficiently mobile to expand and form the faulted loops necessary for twin formation. On the other hand, with thermally-induced recrystallization, the temperature is in the right regime (450-650° C) where the mobility of the leading partial is sufficiently greater than that of the trailing partial so that the twinning mechanism can operate.

In brief, twins will form in ion-implanted silicon if it passes through the temperature range ~400-650° C because of the likely presence of pinned segments of screw dislocations which can be under relatively high shear stresses. This is irrespective of the manner by which this temperature range is reached, i.e. by post-implantation anneal, dynamic anneal, ion-induced recrystallization, or any other means.

3.4 Oxygen Precipitation in Silicon

The formation of precipitates and lattice defects in heat-treated silicon which is supersaturated with interstitial oxygen has received a lot of attention recently. One reason is because the technologically important Czochralski silicon contains about 10^{24} oxygen atoms/m^3. When this material is annealed, a variety of precipitates and lattice defects form which have been studied quite intensively by TEM. The morphology of the defects depend on the time-temperature domain of annealing; for a recent review, see e.g. Bender [53]. For annealing at high temperatures ($>800^\circ$ C) the structure of the defects and precipitates is relatively well understood. However at low to intermediate temperatures (~450-750° C), there are some controversial problems; one source of this is because some of the precipitates are probably metastable phases which complicate the problem. The defect which is relevant to this paper is the so-called "rod-" or "ribbon-like defect" (RLD) which is elongated along a <011> direction. Typically, an RLD has a length of ~1 μm and a cross-section of 1x6 nm^2, i.e. it has a remarkably high aspect ratio of 10^3-10^4. In the HREM images of this defect a kind of two-layer periodicity in the elongated <011> direction may be detected. This would imply that the RLD has a (nano-)crystalline structure. It has a dilational strain field

(interstitial) with a displacement vector of f<100> where $f \sim 0.3a_{si}$. At intermediate annealing temperatures (~650° C), the interface between the RLD and the dc silicon is mostly parallel to the $\{100\}_{dc}$ plane but, sometimes, it has a zigzag shape with small segements parallel to $\{3\bar{1}1\}_{dc}$ and, less frequently, parallel to $\{4\bar{1}1\}_{dc}$ and $\{5\bar{1}1\}_{dc}$ [54]. In this temperature range, segments of RLD often alternate with segments of 60° and 90° dislocation dipoles all collinear along the same <110> rod defect. At lower temperatures (≈485° C), the crystalline structure of the RLD is less clear in HREM images and its habit plane is parallel to $\{3\bar{1}1\}_{dc}$ planes with indications of continuing growth along {100} [55].

Because of the correlation of the loss of oxygen during annealing and the formation of RLDs, Bourret et al. [54] assumed that this crystalline phase is probably a silica phase. Based on this hypothesis, they found a good match between the experimental periodicities of RLDs (from optical diffractograms) and those of coesite, a high-pressure phase of SiO_2 with a monoclinic structure. A comparison of the experimental HREM images of RLDs and the simulated images of coesite also confirmed this assumption. This was further verified by Bender [53] who independently repeated the image matchings and found good correlation between computed images of coesite and HREM images of RLD. This attractive suggestion was taken on by a number of workers because it readily accounted for the increase in the density of RLD defects with annealing time, and the simultaneous loss of interstitial oxygen [55,56]. In fact quantitative estimates of the number of oxygen atoms in the ribbons is in reasonable agreement with infrared data on the loss of oxygen from the solution indicating that the oxygen atoms have formed coesite precipitates [55,57]. However, because of the low annealing temperature, specially at ~485° C, identification of RLD with coesite requires an enhanced oxygen diffusion in silicon. Such an enhancement was, in fact, suggested earlier by Stavola et al. [58] in order to explain their dichroic experiments. Many different mechanisms were suggested to explain the latter set of experiments (for a review see [59]).

Recently, Newman et al. [60] have re-interpreted the dichroic experiments and questioned the enhanced oxygen diffusivity of silicon. In this case, the formation of coesite at low temperatures would not be tenable. Bourret [61] re-examined the evidence for coesite and, based on the similarity of the HREM images of RLDs to those of hexagonal silicon in [62], he suggested that the RLD is in fact dh Si. Another factor in this re-interpretation is the appearance of zig-zag type defects in electron- or ion-irradiated specimens at elevated temperatures with {113} habit planes. This interpretation of RLDs as being dh Si has been also supported by Bender and Vanhellemont [63].

As far the authors are aware, no-one has reported formation of twins in annealing of Czochralski silicon. It is thus concluded that this hexagonal silicon cannot form by the mechanisms proposed in the present series of papers. If the RLD is, in fact, hexagonal silicon, a completely different mechanism would be operative. It has been suggested that dh Si forms by the aggregation of Si self-interstitials which are created during the formation of oxygen precipitats [61]. The details of this process, however, have not been given. This is rather surprising because, as mentioned before, Si_{dh} phase is not thermodynamically favored. Also if dh silicon does form by a different mechanism, it is hard to envisage that it will choose the unexpected orientation relationship of $(0\bar{1}1)_{dc} || (0001)_{dh}$, $[011]_{dc} || [\bar{1}2\bar{1}0]_{dh}$; it would be preferential to have the more natural orientation

relationship $(111)_{dc} || (0001)_{dh}$, $[1\bar{1}0]_{dc} || [11\bar{2}0]_{dh}$. In addition, unlike the RLD (interstitial with b≈f<100>), hexagonal silicon does not appear to produce a dilational effect in any direction, i.e. it is not an interstitial defect. Hence in the opinion of the present authors, the nature of RLD is an open question at the moment. It is probably not coesite, which is not a thermodynamically stable phase at the conditions of RLD formation. And, although there is increasing evidence that Si self-interstitials are necessary for the formation of RLDs [64], it is probably not hexagonal silicon since this requires the existence of correct shear stresses for deformation twinning.

3.5 Deformation of Si under Superimposed Hydrostatic Pressure

It is well known that in the presence of hydrostatic pressure, the brittle/ductile transition temperature can be shifted to lower temperatures. This is of course basically what happens in indentation experiments where the indenter itself produces a hydrostatic component as well as a shear one. Using superimposed confining pressures of ~1500 MPa, Castaing et al. [65] succeeded in plastically deforming silicon at temperatures as low as 300° C. Preliminary TEM observations of the specimens deformed at temperatures below 500° C revealed a high density of microtwins, twins, and stacking faults [65]. These were produced by large resolved shear stresses of up to ~1000 MPa [65] which is much larger than the stress necessary to overcome the stacking fault energy of Si and separate the leading from the trailing partial dislocation [10].

A more thorough microstructural investigation of silicon deformed at low temperatures under hydrostatic pressure was later made by Demenet et al. [66]. They observed a large difference in twin density with respect to the compression axis. In contrast to a high density of twins when the specimen was oriented for multiple glide (compression axis <100>), the twin density was very low when the specimen was deformed under single glide conditions (compression axis <213>). This is of course compatible with the mechanism proposed in [10] because, as mentioned before, two of the requirements for twinning are a pinned segment of screw dislocation and reasonable resolved shear stresses on the primary *and* a cross-slip plane. For single glide condition, cross-slip is negligible and because, at least up to the upper yield point, most of the dislocation are on the primary glide plane, there are not many intersecting dislocation from other slip planes which pin a primary screw dislocation. When the specimens are deformed to higher strains, (past the lower yield point) other slip planes are activated and then some incidence of microtwinning is observed [66]. For specimens oriented for multiple glide, all the necessay conditions, i.e. cross-slipping and pinned screw dislocations, are present and there is a high incidence of twinning. It should also be noted that dislocation velocity is stress dependent and, as Demenet et al. [66] have noted, for <213> orientation the resolved shear stress on the trailing partial is larger than that on the leading partial while in the case of <100> axis compression the reverse is true.

An interesting aspect of the work of Demenet et al. [66] was the observation of hexagonal silicon deformed at 700° C along a <213> axis under a confining pressure of 700 MPa. In these experiments very large resolved shear stresses (~320 MPa) were applied resulting in large strains of ~0.25. The strain corresponds to the end of stage II of the stress-strain curve of silicon where the dislocations rearrange to form cellular structures [66]. Significantly twins, and also very

small quantities of hexagonal silicon, were observed with the latter having the same habit plane and orientation relationship as in eqn. (3). The fact that deformation was carried out to such a high strain implies the activation of many slip systems resulting in pinned segments of screw dislocations. Dislocation interactions in the heavily dislocated material also cause internal resolved shear stresses for cross-glide. The confining pressure presumably may result in some changes in the mobility of partial dislocations, or there may be a higher propensity for pinning of trailing partial dislocations as compared to the leading ones in the heavily dislocated shear bands of the cellular structure. In any case, the final result is the incidence of twinning at the high temperature of 700° C. It should be noted that in the absence of confining pressure, there is no reported incidence of twinning under conditions of single glide at this temperature. The significance of cellular structure is that the twins are localized in the shear bands and twin intersections are more likely with the consequent production of hexagonal silicon.

ACKNOWLEDGEMENT

Useful discussions with Professor G. Welsch on ion-implantation are acknowledged. The work of U. D. and K. H. W. was supported by the Director, Office of Energy Research, Office of Energy Sciences, Materials Sciences Division of the U.S. Department of Energy under contract DE-AC03-76SF00098.

* Present address: Department of Materials Engineering, Technion, Haifa, 32000 Israel.

REFERENCES

[1] P. Pirouz, R. Chaim, U. Dahmen, and K. H. Westmacott, Submitted to Acta Metall. (1989).

[2] U. Dahmen, K. H. Westmacott, P. Pirouz, and R. Chaim, Submitted to Acta Metall. (1989).

[3] A. J. Bogers and W. G. Burgers, Acta Metall. **12**, 255 (1964).

[4] E. C. Bain, Trans. AIME **70**, 25 (1924).

[5] G. Kurdjumov and G. Sachs, Zeits. Physik **64**, 637 (1930).

[6] G. B. Olson and M. Cohen, Met. Trans. 7A, 1905 (1976).

[7] M. Ahlers, Z. Metallk. **65**, 636 (1974).

[8] F. E. Fujita, Met. Trans. **8A**, 1727 (1977).

[9] S. Mendelson, ICOMAT '79, p. 100.

[10] P. Pirouz, Scripta Met. **21**, 1463 (1987).

[11] K. Wessell and H. Alexander, Phil. Mag. **35**, 1523 (1977).

[12] P. Pirouz, R. Chaim, and U. Dahmen, Mat. Res. Soc. Symp. Proc., **104**, 133 (1987).

[13] J. F. Cannon, J. Phys. Chem. Reference Data **3**, 797 (1974).

[14] J. Z. Hu, L. D. Merkle, C. S. Menoni, and I. L. Spain, Phys. Rev. B, **34**, 4779 (1986).

[15] S. Minomura and H. G. Drickamer, J. Phys. Chem. Solids **23**, 451 (1962).

[16] J. C. Jamieson, Science **139**, 762 (1963).

[17] R. H. Wentorf and J. S. Kasper, Science **139**, 338 (1963).

[18] J. S. Kasper and S. M. Richards, Acta Cryst. **77**, 752 (1964).

[19] H. Olijnyk, S. K. Sikka, and W. B. Holzapfel, Physics Letts. **103A**, 137 (1984).

[20] J. Z. Hu and I. L. Spain, Solid State Commun. **51**, 263 (1984).

[21] M. T. Yin and M. L. Cohen, Phys. Rev. Lett. **45**, 1004 (1980).

[22] M. T. Yin and M. L. Cohen, Phys. Rev. B **26**, 5668 (1982).

[23] M. T. Yin, Phys. Rev. B **30**, 1773 (1984).

[24] C. Frondel and U. B. Marvin, Nature **214**, 587 (1967).

[25] E. I. du Pont de Nemours and Company, Netherland Patenty Release Nop. 6506395, November 22, 1965.

[26] F. P. Bundy and J. S. Kasper, J. Chem. Phys. **46**, 3437 (1967).

[27] K. Lonsdale, The Am. Mineralogist **56**, 333 (1971).

[28] R. E. Hanneman, H. M. Strong and F. P. Bundy, Science **155**, 995 (1967).

[29] V. G. Eremenko Sov. Phys. Solid State **17**, 1647 (1976).

[30] V. G. Eremenko, Sov. Phys. Solid State **13**, 230 (1971).

[31] V. G. Eremenko and V. I. Nikitenko, Phys. Stat. Sol. (a) **14**, 317, (1972).

[32] M. L. Rudee and A. Howie, Philos. Mag. xx, 1001 (1972).

[33] J. R. Parsons and C. W. Hoelke, Nature, **301**, 591 (1983).

[34] J. R. Parsons and C. W. Hoelke, Phil. Mag. A, **50**, 329 (1984).

[35] T. Y. Tan, H. Foll, and S. M. Hu, Phil. Mag. A **44**, 127 (1981).

[36] G. F. Cerofolini, L. Meda, G. Queirolo, A. Armigliato, S. Solmi, F. Nava, and G. Ottaviani, J. Appl. Phys. **56**, 2981 (1984).

[37] F. F. Komarov, A. P. Novikov, T. T. Samoilyuk, V. S. Solov'yev, and S. Yu. Shiryaev, Radiat. Eff., **90**, 307 (1985).

[38] M. Servidori, S. Cannavio, G. Ferla, A. La Ferla, S. U. Campisano, and E. Rimini, Nucl. Instrum. Methods Phys. Res. B **19/20**, 317 (1987).

[39] M. Servidori, S. Cannavio, G. Ferla, A. La Ferla, and E. Rimini, Appl. Phys. A **44**, 213 (1987).

[40] G. H. Schwuttke, K. Brack, E. F. Gorey, A. Kahan, L. F. Lowe, and F. Fuller, Phys. Stat. Sol. (a), **14**, 107 (1972).

[41] I. Ohdomari and N. Onoda, Philos. Mag. **35**, 1373 (1977).

[42] D. J. Mazey, R. S. Nelson, and R. S. Barnes, Phil. Mag., **17**, 1145 (1968).

[43] A. Golanski, A. Fiderkiewicz, H. Rzewuski, M. Lefeld-Sosnowska, J. Gronkowski, R. Grotzschel, U. Kreissig, and H. Bartsch, Phys. Stat. Solidi (a), **38**, 139 (1976).

[44] R. G. Elliman, J. S. Williams, W. L. Brown, A. Leiberich, D. M. Maher, and R. V. Knoell, Nucl. Instrum. Meth. Phys. Res. B **19/20**, 435 (1987).

[45] L. Cspregi, J. W. Mayer, and T. W. Sigmon, Appl. Phys. Lett., **29**, 92 (1976).

[46] L. Cspregi, E. F. Kennedy, T. J. Gallagher, J. W. Mayer, and T. W. Sigmon, J. Appl. Phys. **48**, 4234 (1977).

[47] L. Cspregi, E. F. Kennedy, J. W. Mayer, and T. W. Sigmon, J. Appl. Phys. **49**, 3906 (1978).

[48] N. N. Gerasimenko, A. V. Dvurechensky, G. A. Kachrin, N. B. Pridachin, and L. S. Smirnov, Sov. Phys. Semicond., **6**, 1588 (1973).

[49] A. V. Dvurechensky, N. N. Gerasimenko, S. I. Romanov, L. Smirnov, Radiat. Eff. **30**, 69 (1976).

[50] F. F. Komarov, V. S. Solov'yev, and S. Yu Shiryaev, Radiat. Eff., **42**, 169 (1979).

[51] A. George and J. Rabier, Revue Phys. Appl., **22**, 941 (1987).

[52] E. P. EerNisse, in "Ion Implantation in Semiconductors and other Materials", ed. B. L. Crowder, New York: Plenum Press, pp 531-540 (1973).

[53] H. Bender, Phys. Stat. Sol. (a), **86**, 245 (1984).

[54] A. Bourret, J. Thibault-Desseaux, and D. N. Seidman, J. Appl. Phys. **55**, 825 (1984).

[55] W. Bergholz, J. L. Hutchison, and P. Pirouz, J. Appl. Phys. **58**, 3419 (1985).

[56] W. Bergholz, P. Pirouz, and J. L. Hutchison, J. Electron. Mater. **14a**, 717 (1984).

[57] W. Bergholz, J. L. Hutchison, and P. Pirouz, Inst. Phys. Conf. Ser. No. **76**, 11, (1985).

[58] M. Stavola, J. R. Patel, L. C. Kimmerling, and P. E. Freeland, Appl. Phys. Lett., **42**, 73 (1983).

[59] A. Ourmazd, W. Schroter, and A. Bourret, J. Appl. Phys., **56**, 1670 (1984).

[60] R. C. Newman, Mat. Res. Soc. Symp. Proc., **104**, 25 (1988).

[61] A. Bourret, Inst. Phys. Conf. Ser. No. **87**, 39, (1987).

[62] P. Pirouz, R. Chaim, and J. Samuels, Izvestiya Nauk Akademiya S.S.S.R. **51**, 753 (1987).

[63] H. Bender and J. Vanhellemont, Phys. Stat. Sol. (a), **107**, 455 (1988).

[64] M. Reiche and W. Nitzsche, Proc. GADSET, Garzau, GDR, 98 (1987).

[65] J. Castaing, P. Veyssier, L. P. Kubin, and J. Rabier, Philos. Mag. A **44**, 1407 (1981).

[66] J. L. Demenet, J. Rabier, and H. Garem, Inst. Phys. Conf. Ser. No. **87**, 35 (1987).

LAWRENCE BERKELEY LABORATORY
TECHNICAL INFORMATION DEPARTMENT
1 CYCLOTRON ROAD
BERKELEY, CALIFORNIA 94720